# The Role of Telomeric Heterochromatin in Regulating Telomere Length Maintenance and Stability

**Shreya Shrestha**

**April 3, 2024**

**Departmental Honors Thesis**

**Department of Molecular, Cellular, and Developmental Biology**

**College of Arts and Sciences**

**University of Colorado Boulder**

**Thesis Advisor: Nausica Arnoult, PhD**

Department of Molecular Cellular & Developmental Biology

**Council Representative: Cheryl Pinzone, PhD**

Department of Molecular Cellular & Developmental Biology

**Outside Reader: Alexandra Whiteley, PhD**

Department of Biochemistry

**ACKNOWLEDGEMENTS**

I would like to thank my professor, mentor, and honors thesis advisor, Nausica Arnoult, for granting me this opportunity to develop my research skills and apply my molecular biology knowledge in a practical setting. Her dedication to the sciences and the joyous energy she brings to lab has been a constant source of inspiration throughout my time in college.

I also give my sincerest thanks to Erin Taylor for her incredible mentorship, her support with this thesis, and her endless words of encouragement in lab and in life over these past three years. I credit my proficiency in scientific skills and writing to her teachings.

I would like to extend my gratitude to all other members in the lab, including Bruce Proctor, Raquel Ortega, Ben Nebenfuehr, Kerri Ball, and Shane Brelinski, for the innumerable ways in which they have helped me navigate the lab and pushed me to be a better scientist.

I would like to give a special thanks to Akarea Steele and Giorgio Matessi for their constant love and support.

Finally, I would like to thank my family, Yogesh, Vinu, Priyaj, and Neerav, for being the reason for everything I do.

**ABSTRACT**

Telomeres are protective structures that preserve genome integrity and stability by preventing chromosome end degradation and misrecognition as DNA damage sites. Dysregulation of telomere structure or length maintenance can have drastic consequences on overall telomere stability, often leading to premature aging diseases or the development of cancer. Though the structural and functional components of telomeres, including the telomere-binding protein complex shelterin, have been well-established, the role of chromatin in maintaining telomere stability remains elusive. Here we investigate the potential role of constitutive heterochromatin using a protein-tethering approach to enrich features of heterochromatin specifically at telomeres. Our results show that telomeric enrichment of the heterochromatin-associated trimethylation of histone 3 on Lysine 9, H3K9me3, does not result in substantial telomere deprotection. Conversely, enrichment of heterochromatin protein 1 (HP1α), of a different heterochromatin feature, produces significant DNA damage and telomere dysfunction. Using fluorescent microscopy techniques, we measured telomere length, replication stress, and levels of telomeric DNA damage after heterochromatin enrichment at telomeres. We demonstrate that cells with telomeric enrichment of HP1α exhibit increased DNA damage at telomeres, diminished telomere length, as well as bridging of telomeres between multiple nuclei, indicative of telomere entanglements. These phenotypes suggest that heterochromatin is detrimental, rather than protective, to normal telomere function. Interestingly, a subset of cancer cells, , which maintain their telomeres through a mechanism called Alternative Lengthening of Telomeres (ALT), rely on HP1a for viability and are known to have high levels of heterochromatin, replication stress, recombination, and DNA damage at their telomeres. The observed telomere dysfunction in non-ALT cells upon HP1a enrichment at telomeres may provide insight into the

role of HP1α in the ALT pathway and may thus inform the future development of anti-cancer drug therapies.

## INTRODUCTION

Telomeres are evolutionarily conserved nucleoprotein structures at the terminal ends of linear chromosomes in most eukaryotic organisms. Mammalian telomeres are composed of TTAGGG tandem repeats and a single-stranded G-rich 3' overhang. The ends of linear chromosomes pose two critical issues for the cell. The first, known as the end-protection problem, arises because terminal ends closely resemble DNA double-stranded breaks (DSBs). The cell has evolved highly regulated DNA damage repair (DDR) mechanisms essential for preserving genome integrity. However, activating DDR machinery at telomeres results in cell cycle arrest, chromosome end-to-end fusions, or sequence exchanges (de Lange, 2005). The cell must take measures to escape these consequences and protect itself against the DDR response at chromosome ends. This is the primary function of shelterin, a complex of six non-histone proteins that includes TTAGGG-binding subunits, TRF1 and TRF2. Shelterin specifically binds telomeric sequences and facilitates the formation of telomere-loops (or t-loops), enabling strand invasion of the 3' overhang into telomeric duplex sequences to hide the chromosome end and thereby inhibit DDR signaling and nucleolytic degradation (Figure 1/2C) (Arnoult 2015). TRF2 suppression results in the loss of the t-loop and accumulation of DDR proteins, including 53BP1, y-H2AX, and phosphorylated ATM S1981-P (de Lange, 2005).

The second molecular challenge specific to chromosome ends is the end-replication problem. Due to the anti-parallel nature of DNA replication, classical polymerases cannot replicate

chromosomes until the very end on the lagging strand, leading to the loss of tens of terminal DNA bases. After replication, chromosome ends are processed by exonucleases to form the G-rich overhang that is essential to t-loop formation. As a result, chromosome ends progressively shorten with each round of cell division. However, the presence of the TTAGGG tandem repeats over tens of kilobases prevents the potential loss of essential genetic information. Over time, normal dividing cells accumulate short telomeres that lose their protective function as a result of an inability to bind shelterin and form t-loops, such that chromosome ends are recognized as sites of DNA damage and targeted by DDR machinery (Figure 1). Eventually, these events cause the cell to enter replicative senescence if damage checkpoints are in place, or otherwise elicit a response for cell death (de Lange 2005).

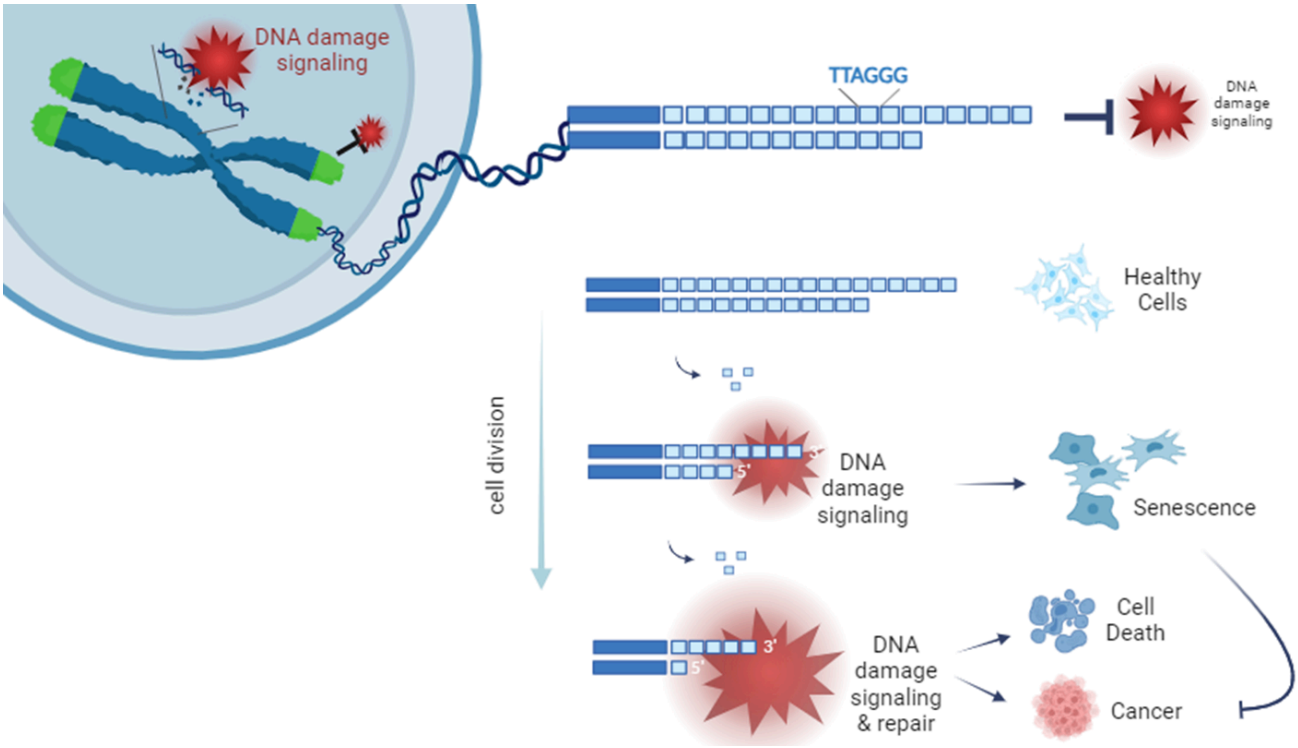


**Figure 1: The end-replication problem has profound consequences on telomere stability and cell fate.** Incomplete replication at chromosome ends leads to progressive telomere shortening. Upon reaching a certain length threshold, very short telomeres activate a DNA damage response, which can lead to senescence, apoptosis, and in some cases, cancer development.

In the germ line and stem cells, this progressive telomere shortening is compensated by the shelterin-mediated recruitment and activation of telomerase, a specialized ribonucleoprotein reverse transcriptase that uses a complementary intrinsic RNA template to bind the 3' overhang and elongate telomeres (Bonnell 2021). By processively synthesizing telomeric repeats to the 3' strand with subsequent polymerase fill-in, telomerase maintains telomere length in a cell cycle-dependent manner, delaying senescence and prolonging the cell's proliferative lifespan (Lim 2021).

Telomerase is active in germline cells and other highly dividing cells, such as human T cells, skin cells, and bone marrow. In normal adult somatic cells, however, telomerase is typically silenced so that aging cells, which tend to accumulate mutations over time, cannot continue dividing, and therefore cannot cause physiological harm. The heavily regulated process of telomere length maintenance is essentially a molecular "clock" that contributes to natural tissue aging and operates as an important *in vivo* tumor suppressor (Shay 2009). To gain unlimited proliferative potential, cancer cells need to circumvent this mitotic clock. They do so by activating a mechanism for telomere elongation. The reactivation of telomerase in somatic cells is one of two telomere maintenance mechanisms that allows cancer cells to overcome proliferative barriers (Roake 2020). The gene responsible for producing the catalytic subunit of telomerase, known as human *TERT* or *hTERT*, was discovered to be silenced in most normal cells, yet constitutively expressed in cancer cells (Chan 2002). Thus, telomerase reactivation and upregulation were rapidly accepted to be a key biomarker of cancer development in approximately 85% of cases, making telomerase an attractive target for drug therapies. However, several obstacles, including the slow, incremental nature of telomere shortening over many cell

cycles, have hampered the success and practicality of past clinical attempts to develop telomerase inhibitors (Guterres 2020).

In the remaining ~10-15% of cancers where telomerase is absent, telomeres use an independent telomere maintenance mechanism, called alternative lengthening of telomeres (ALT), in which a telomeric DNA template is used to replicate a telomere of a non-homologous chromosome, a process known as break-induced replication (Rose 2023). ALT cells display an array of unusual traits, including extrachromosomal telomeric sequences in the form of double-stranded telomere circles (t-circles) and partially single-stranded C-circles, among others. Chromosomal and extrachromosomal telomeric DNA and homologous recombination factors frequently colocalize with promyelocytic (PML) nuclear bodies, commonly referred to as ALT-associated PML bodies (APBs) in the context of ALT+ cancer cells (Cesare 2010). Other defining characteristics of ALT activity include telomere clustering, highly heterogeneous telomere length, and high levels of recombination and telomere sister chromatid exchange (Zhang 2020). These features indicate severe genome instability and pose considerable challenges for telomere end protection and length dynamics. Though the phenotype and functions of ALT are well-studied, mechanisms to regulate the pathway remain unclear.

Replication of telomeric sequences is particularly challenging, owing to the formation of DNA secondary structures like t-loops, as well as DNA-RNA hybrids that form by the association of telomeric DNA with Telomeric repeat-containing RNAs (TERRA), the long non-coding RNA transcribed at telomeres (Azzalin 2007). Telomeric sequences can also fold into four-stranded DNA structures, called G-quadruplexes, due to their repetitive, G-rich nature (Tan 2020). These

unique structures at telomeres pose mechanical challenges that complicate the unwinding and replication of DNA strands, resulting in the stalling or arrest of replication fork progression, known as replication stress. Under fluorescent microscopy analysis of chromosomes, replication stress can be observed in the presence of fragile telomeres, which are structural aberrations that deviate from the typical circular telomere probe signal when analyzing telomeres of metaphase chromosomes by Fluorescence In-Situ Hybridization (FISH) (Yang 2020). This phenotype was defined in a seminal paper in which the authors performed a TRF1 knockdown experiment and observed a sharp increase in abnormal telomeric signal morphology, or fragile telomeres. Their subsequent replication analysis of DNA fibers demonstrated that TRF1 is essential for the prevention of replication stress at telomeres. Thus fragile telomeres are a hallmark phenotype for replication stress events (Sfeir 2009).

In addition to aberrant morphology, the loss of telomere FISH signal at chromosome ends, known as free ends, is also considered an indication of replication stress. This is because the processing of replication stress at telomeres often results in rapid telomere loss. Abnormally high levels of replication stress trigger the reactivation of telomere maintenance mechanisms in cancer cells (Lu 2022). Furthermore, studies indicate that ALT+ cells are especially prone to replication stress, and proteins involved with managing replication stress may be non-canonically recruited at ALT telomeres (Shen 2021). Replication stress events are associated with accelerated telomere shortening and early onset of replicative senescence, which, as mentioned above, are major sources of genomic instability that can be linked to tumorigenesis (Arnoult 2015). For this reason, studies on telomere regulation often use replication stress as a metric for general

telomere stability, providing researchers with a valuable tool to investigate the potential effects of different features at telomeres.

The general functions of telomere end protection and length maintenance have been well-characterized, especially regarding the involvement of the shelterin protein complex. However, the ability of shelterin to bind to telomeric DNA, and thus the preservation of telomere stability, depends intrinsically on higher-order chromatin structure. The specific effects of chromatin on telomere structure and function remain unclear. Eukaryotic DNA is wrapped around histone octamers, each containing two copies of H2A, H2B, H3, and H4, to form nucleosomes that can be folded and positioned to form higher-order chromatin structures (Soman 2022). At telomeres, histone-mediated interactions of nucleosomes cause them to stack together to form columnar structures. These structures may be further organized into loosely compacted (open) transcriptionally active euchromatin, or tightly compacted (condensed), transcriptionally repressive heterochromatin (Xu 2020). Heterochromatin can be divided into two types: facultative heterochromatin, which is more dynamic and generally regulates gene expression, and constitutive heterochromatin, which is typically found at highly repetitive genome loci, such as pericentromeric repeats, and is therefore constant between cell types.

DNA at telomeric regions was originally considered constitutively heterochromatic, as characterized by the enrichment of trimethylated histone H3 (H3K9me3), though recent developments have introduced controversy to this claim (Cubiles 2018). Constitutive heterochromatin was first found to be localized to pericentromeric and telomeric regions in *Drosophila melanogaster*, budding yeast, and mouse embryonic stem cells, and thereby assumed

to be a conserved characteristic of all telomeres (Vaquero-Sedas 2011). However, new studies using chromatin-immunoprecipitation (ChIP) sequencing in human cells challenge this assumption, proposing an alternative theory that human telomeres in normal cells are not enriched in H3K9me3, but that ALT+ cells display heterochromatic levels of H3K9me3 enrichment (Gauchier 2019). Mammalian genomes also contain HP1 homologs, HP1α, HP1β, and HP1$\gamma$, proteins that localize to heterochromatin and are involved in chromatin compaction and gene silencing (Janssen 2018). HP1α is specifically recruited to H3K9m3, and its binding stimulates local heterochromatin spreading by recruiting histone methylase SETDB1 to further enrich H3K9me3 in a feedforward loop. Furthermore, HP1α is necessary to activate ALT mechanisms, and inhibition of SETDB1 results in the loss of ALT phenotypes (Gauchier 2019). The associations between HP1α, heterochromatin, and telomere maintenance have yet to be fully established.

Despite being a central structural component of telomeres, the nature of telomeric chromatin and its function in regulating telomere stability remains controversial. We seek to address this knowledge gap in the field of telomere biology by experimental modulation of heterochromatic features and analysis of their effects at telomeres. We used overexpression of engineered transgene fusion proteins to recruit proteins that promote or spread histone methylation, thereby upregulating heterochromatin in a controlled system. By this method of molecular tethering, we enriched HeLa telomeres in H3K9me3 or HP1α and observed the effects on telomere stability, namely the levels of DNA damage and structural abnormalities. Fluorescent microscopy analyses revealed that enrichment of HP1α significantly increased levels of DNA damage and rapid telomere shortening. Our findings suggest that the modulation of heterochromatin states may

play a role in the regulation of telomere end-protection and length maintenance, providing new insights into the relationship between telomeric chromatin structure in both normal and pathological states.

## RESULTS

### Design and verification of model for telomere-specific H3K9me3 overexpression

To study the effects of modified heterochromatin levels at telomeres, we designed a model system to enhance the heterochromatin mark H3K9me3 specifically at telomeres by creating a doxycycline-inducible TRF1 fusion protein construct with the minimal domain of the DNA binding Krüppel-Associated Box (KRAB) zinc finger protein. The minimal KRAB domain is a powerful molecular biology tool typically used to promote transcriptional repression and epigenetic gene silencing by binding KRAB-associated protein 1 (KAP1). KAP1 subsequently recruits histone methylases like SETDB1 to promote H3K9me3 and heterochromatin enrichment (Emerson 2009). KRAB domains are typically used for CRISPR inhibition screens, in which KRAB is fused to catalytically inactive Cas9 and directed to promoters to mediate gene silencing by SETDB1 recruitment, H3K9me3 enrichment, and the spreading of heterochromatin (Li 2021).

We fused KRAB to the shelterin component and telomere binding protein TRF1 to specifically enrich heterochromatin at telomeres. TRF1 tethers the KRAB minimal domain to TTAGGG repeats so it can recruit KAP1 and the associated protein complex, including SETDB1 and HP1α, to promote and spread the H3K9me3 heterochromatin mark. The high efficiency and small size of the KRAB domain enable reliable trimethylation of H3 without substantial extraneous disruption to the local environment. As controls, we constructed a plasmid with only

TRF1, as well as a plasmid with TRF1 fused to a mutated KRAB protein (KRABmut) that does not recruit the KAP1 protein complex and thus does not induce H3K9me3 enrichment.

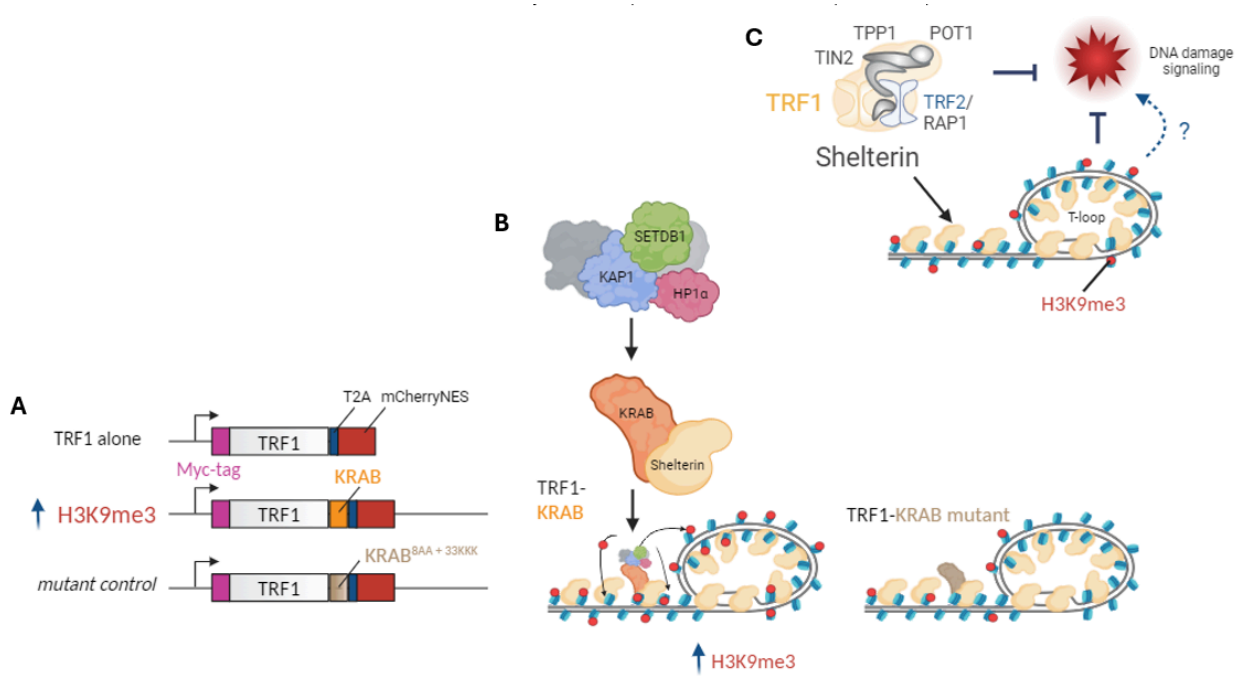


**Figure 2: Plasmid construct for H3K9me3 enrichment.** (A) TRF1 was fused to KRAB to promote H3K9 trimethylation at with telomere locus specificity. Plasmids were driven by a doxycycline promoter and included fluorescent reporters, Myc and T2A-mCherry NES, to verify induction. (B) TRF1-KRAB binds KAP1 to recruit histone methylase, SETDB1, and H3K9me3 reader, HP1α, to enrich H3K9me3 at telomeres. TRF1-KRABmut is structurally mutated to prevent recruitment of this protein complex. (C) Diagram of shelterin, with telomere binding subunit TRF1, and t-loop formation that inhibits the DNA damage response at telomeres.

We included a Myc-tag at the N-terminal end of TRF1 to check for the telomere-specific fusion protein expression by Western blotting and its localization by immunofluorescence. We also added an auto-cleaving T2A signal followed by red fluorescent protein, mCherry, with a nuclear export signal (NES) to verify the induction of our construct by flow cytometry. Upon translation, one mCherry protein will be expressed for every fusion protein expressed, allowing measurements of mCherry signal to be used as a proxy for fusion protein expression. The

addition of the NES on mCherry was included to minimize the risk of background fluorescence in the nucleus in later-stage fluorescent analysis experiments. The fusion construct was placed under a doxycycline-inducible promoter, which functions as an on/off switch for protein expression. When doxycycline is added to the cell culture media, it binds and activates the transcription factor, rtTA, that recognizes the doxycycline-responsive promoter and induces transcription of the fusion construct. This allowed us full control over when the fusion protein was expressed, which was important to produce negative controls for each condition.

The fusion protein construct was cloned into a lentiviral vector. We co-transfected HEK 293T cells with this plasmid and packaging vectors and harvested the virus that we then used for transduction of HeLa cells. The transduced cells were then selected for puromycin resistance, and the +Dox conditions were induced with doxycycline for 72 hours before collection. To analyze protein expression levels in our HeLa cells, we utilized flow cytometry, which allows the passage of single cells through a laser and excites mCherry fluorescence. The levels of mCherry expression, a proxy for fusion protein expression, were plotted to visually analyze the efficiency of induction of our transgene. Figure 3A shows the flow cytometry analysis on TRF1 cells with (right) and without (left) Dox induction, as well as a heatmap representation of the data. Without induction, most cells do not show mCherry fluorescence as expected. However, around 2% of non-induced cells exhibited mCherry expression, indicating minor leakage of the inducible promoter. As seen in the IF FISH of Figure 3B and the heat map 3C, upon induction, mCherry fluorescence can be observed in most cells, though at varying levels.

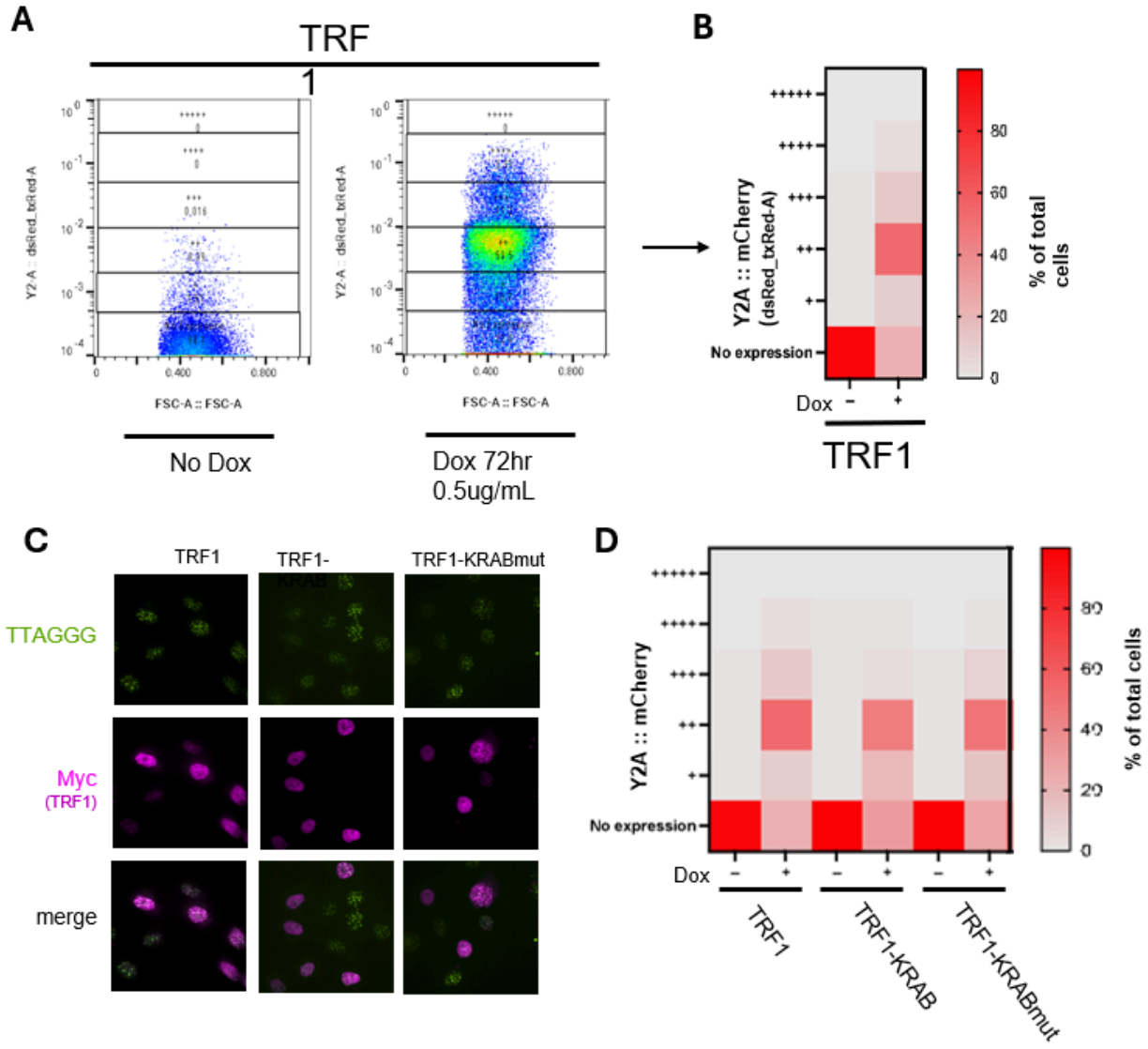


**Figure 3: Heterogeneous expression of fusion protein in HeLa.** (A) Example of FACS analysis of mCherry fluorescence provides visualization of TRF1 fusion protein expression with and without 3-day Dox induction at 0.5 ug/mL concentration. Data is displayed in heat map to compare distribution of expression levels across conditions. (B/C) Representative IF-FISH images of Myc-tagged TRF1 expression and heatmap of flow cytometry data show highly heterogenous induction levels across all Dox-induced conditions.

This suggests that expression of the fusion protein is highly heterogeneous between cells, likely due to the random integration of the fusion construct into the HeLa cell genome that occurs upon transduction with lentivirus. Chromatin state, nearby transcription factors, and various other local

conditions may have affected gene expression at these random points of integration, such that the fusion proteins were unevenly expressed. We sought to equalize induction levels for each condition, because heterogeneous expression of the fusion protein may introduce uncontrolled experimental variability, which would make analysis difficult and results unclear.

To address this experimental issue and obtain tighter control over our fusion protein expression, and thus H3K9me3 enrichment, we wanted to isolate clones with similar levels of expression for consistent induction across conditions. We seeded transduced HeLa cells in 96 well plates at a concentration of 1 cell per well and screened for wells that contained a single cell, which were then grown as clonal lines of uniform genetic background. We analyzed the expression levels of these distinct clonal populations through flow cytometry once more and selected clones with similar levels of expression to use as our experimental cell lines (Figure 4A/B). Homogenous expression and proper Dox induction of all selected subclones were confirmed by IF-FISH (Figure 4C) and Western Blot analysis (Figure 4D) of TRF1 protein concentration, along with verification that global levels of H3K9me3 remained unchanged. Because we are analyzing the effects of heterochromatin upregulation specifically at telomeres, it was important to ensure that the TRF1-KRAB fusion protein was only tethering KRAB at telomeric sequences and promoting H3K9me3 enrichment locally rather than anywhere in the genome. This was verified by the H3K9me3 blot showing relatively equal histone mark levels across all conditions.

**Figure 4: Subcloning results in equivalent expression of fusion protein construct.** (A) Single cells are isolated to produce clonal populations with a uniform genetic background. (B) Heatmap in displaying selected colonies with homogenized fusion protein expression levels. (C) Representative images of Telo-C probe overlaid with Myc antibody displaying equivalent TRF1 levels. (D) Western blot analysis of Myc-tagged TRF1 protein concentratiosn for all conditions with and without Dox, including B-acting loading control and H3K9me3 global expression levels

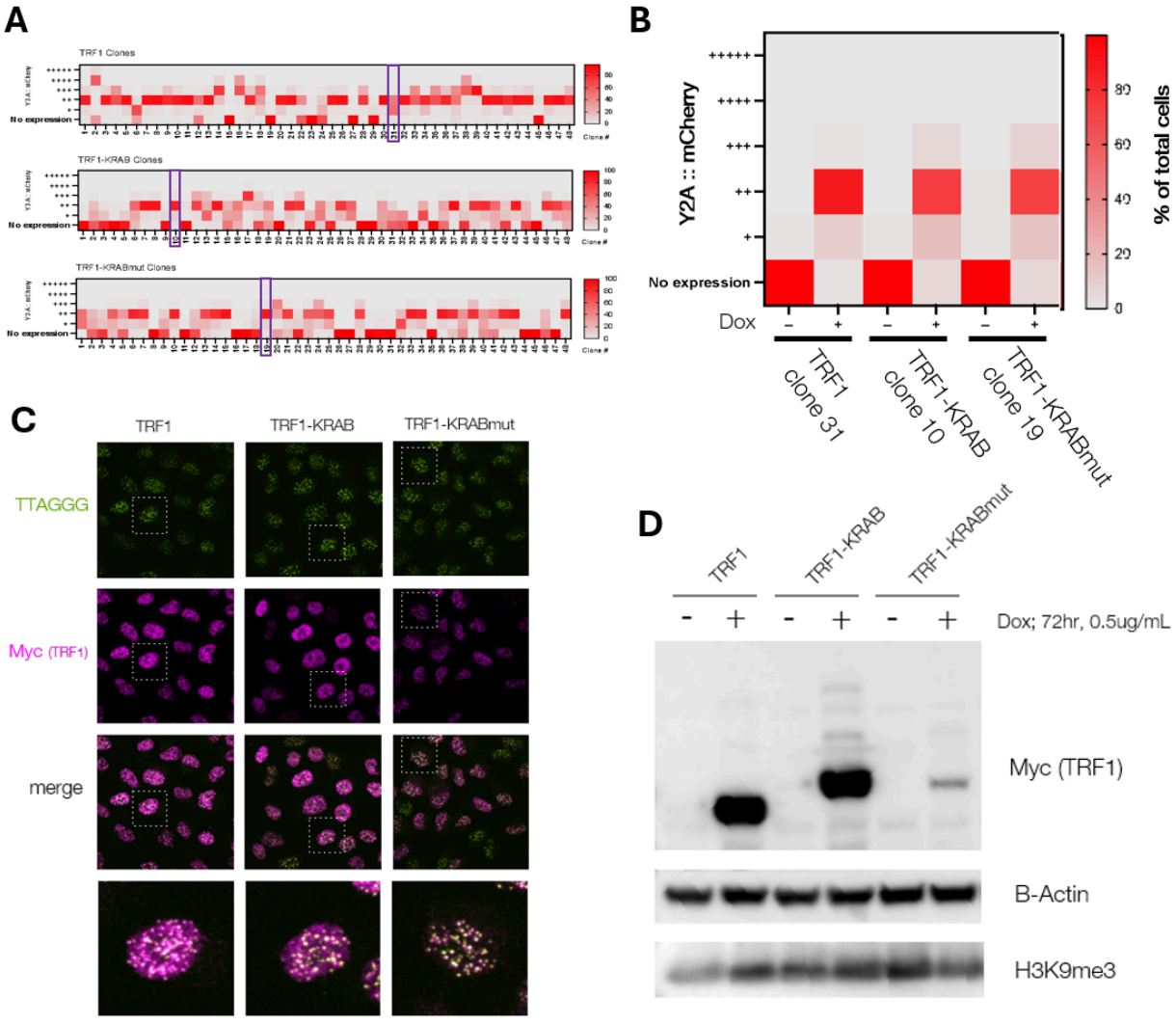

**H3K9me3 enrichment by TRF1-KRAB does not affect telomere features.**

As previously mentioned, we aimed to experimentally enrich heterochromatic features to better understand the role of telomeric chromatin in the regulation of telomere end-protection and length maintenance. We quantified and compared levels of DNA damage at telomeres by Immunofluorescence-FISH (IF-FISH), a method that complements protein-specific fluorescent labeling, with nucleic acid-specific fluorescent labeling to examine colocalization between DNA damage signaling proteins and telomeric sequences, indicating loss of DNA damage signaling inhibition or telomere dysfunction/deprotection. We sought to use this method to determine if H3K9me3 enrichment would result in the accumulation of DNA damage factors, namely key DNA damage protein 53BP1, at telomeres. The frequency of these colocalization events, called Telomere-dysfunction Induced Foci (TIFs), is typically used as a metric of telomeric deprotection. We cultured each condition on coverslips and overlaid them with antibodies directed against 53BP1 and Myc, to verify Dox induction and fusion protein localization, as well as a peptide nucleic acid (PNA) Telo-C probe that binds TTAGGG sequences. We manually quantified TIFs, represented by the colocalization of the 53BP1 signal in the red channel and the telomere probe signal in the green channel. We found that H3K9me3 enrichment by KRAB has a slight but insignificant effect on telomere end-protection compared to wild-type conditions ($p>.05$).

To further establish the potential effects of H3K9me3 upregulation, specifically concerning replication stress, we analyzed metaphase chromosomes with and without KRAB-mediated H3K9me3 enrichment. We used a different specialized FISH protocol for telomeres, known as Telo-FISH. This protocol involves generating metaphase spreads, in which cells are arrested in

metaphase to produce chromosome compaction, swollen via hypotonic shock, fixed, and then dropped onto glass slides so the cell membrane bursts and the chromosomes spread across the surface. The DNA is then denatured and telomeres are hybridized to a PNA Telo-C probe. PNA probes are semiquantitative probes with remarkably high binding affinity to their targets, due to their hydrophobic character and neutral polyamide backbone. This makes the fluorescent signal of PNA hybridization at telomeres a strong proxy for telomere length (Figure 6A). We imaged the resulting FISH metaphases with a spinning confocal disk microscope and counted the number of chromosome ends with no telomere signal, or those with fragile telomeres. As shown in Figures 6B and 6C, we found that expression of TRF1-KRAB had no significant effect on free ends and or fragile telomeres ($p>.05$).

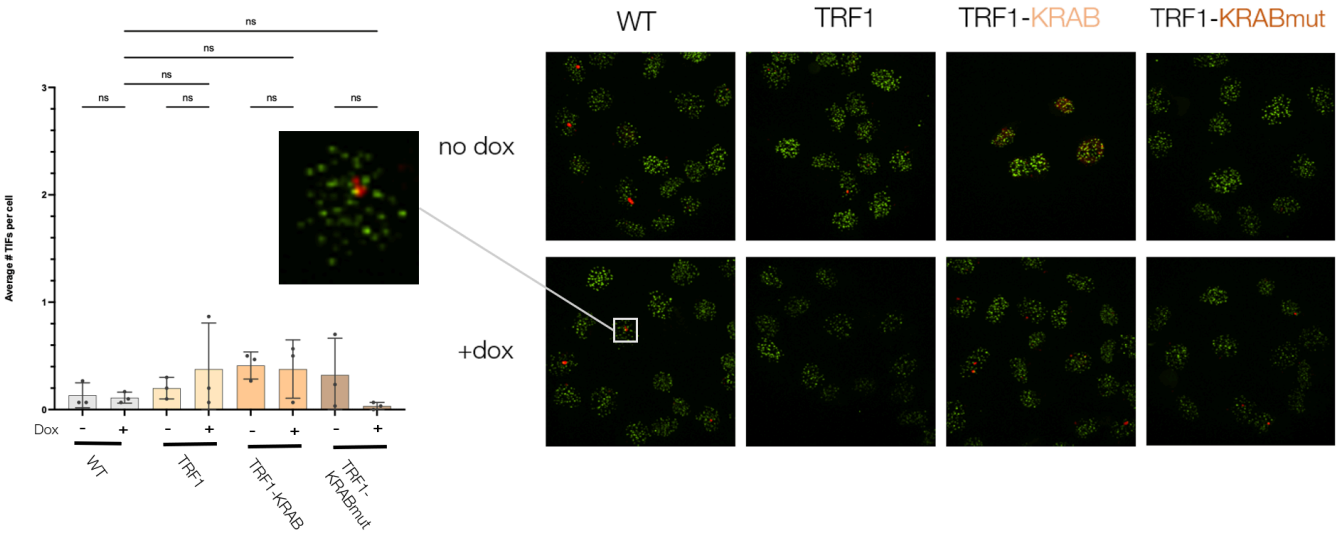


**Figure 5: TRF1-KRAB expression does not affect DNA damage levels at telomeres.** IF-FISH immunostaining to assess colocalization of DNA damage repair (DDR) protein 53BP1 (red) and telomeres (green), indicative of Telomere-dysfunction Induced Foci (TIFs). Left: quantification of average TIFs per cell display no significant change in accumulation of DDR machinery due to KRAB-mediated H3K9me3 enrichment. Right: representative images of all conditions, with example of colocalization event in WT +dox condition.

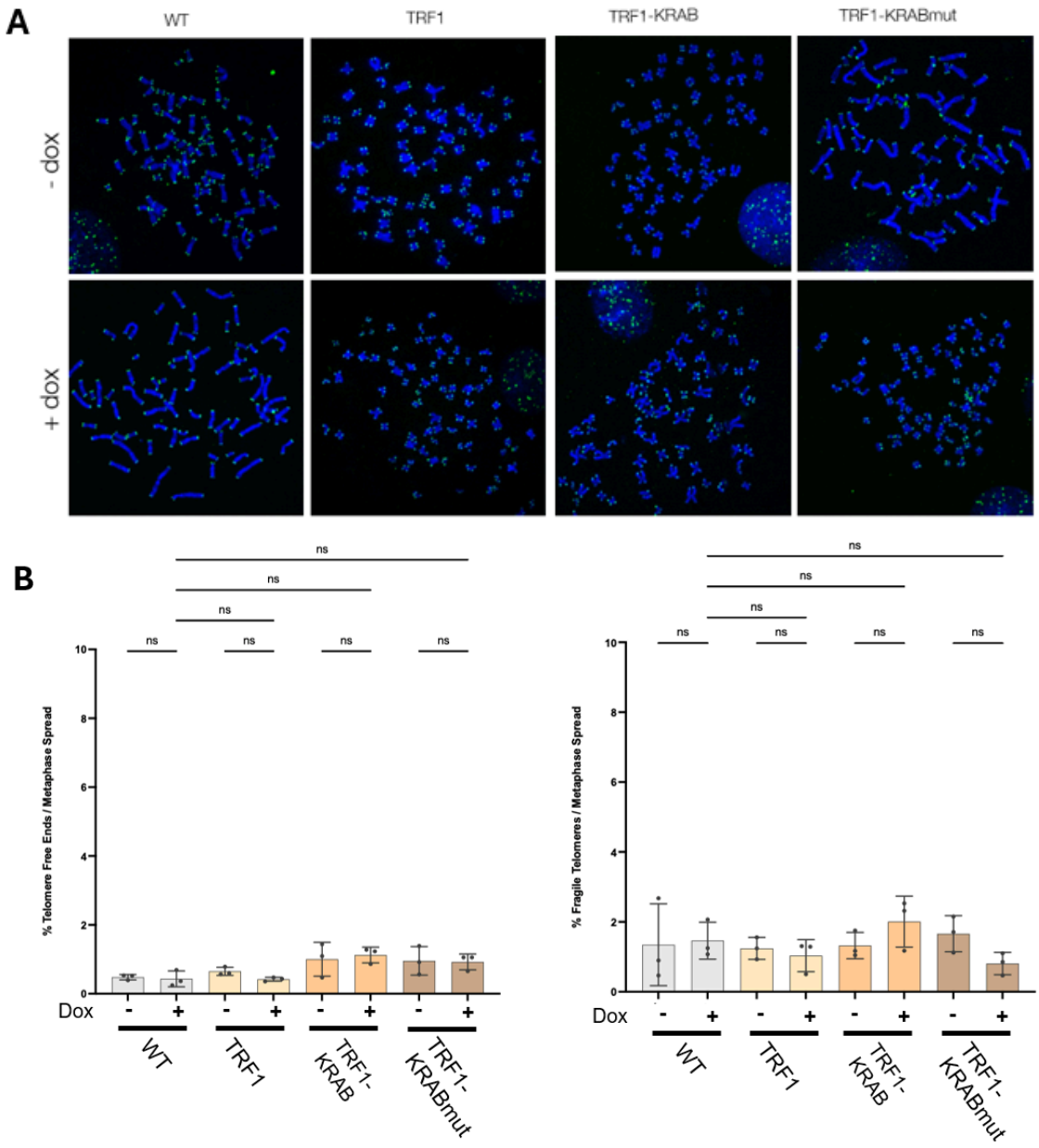


**Figure 6: TRF1-KRAB expression does not affect replication stress telomere length dynamics.** (A) Representative images of Telo-FISH replication stress assay using Telo-C PNA probe (green) counterstained with DAPI (blue). Abnormally-shaped probe signal was quantified as fragile telomeres, or replication stress events, and total loss of telomere signal was quantified as free ends. (B) Left: Quantification of free ends reveals rapid telomere shortening did not occur as a result of KRAB. Right: Fragile telomere quantification reveals no change in replication stress due to KRAB enrichment of H3K9me3.

We reasoned that heterochromatin states are regulated by a combination of factors, and that experimental modulation of H3K9me3 levels may not represent enrichment of all heterochromatic features that could be involved in telomere function. To further understand if constitutive heterochromatin generally serves a function at telomeres, we chose to shift our focus from increasing H3K9me3 density to increasing the presence of its binding partner, HP1α, to determine whether a different heterochromatic feature may affect genomic stability at telomeres.

**Cells enriched in HP1α exhibited substantial DNA damage and telomere instability**

We created a new fusion protein construct for HPα enrichment using the same plasmid design described above, this time fusing TRF1 to HP1α instead of KRAB. Tethering HP1α directly to telomeres would circumvent SETDB1 mediated enrichment of H3K9me3 and HP1α and directly increase HP1α at telomeres. Importantly, we fused TRF1 to a mutated version of HP1α that does not bind H3K9me3, to avoid the recruitment of our fusion protein to every genomic loci enriched in H3K9me3. We again produced clonal lines and selected clones with homogeneous expression (data not shown). We performed IF-FISH analysis on the new HP1α conditions, using the same three primary antibodies as in the KRAB experiments (Figure 7A). Once again, we manually quantified 53BP1 colocalization with telomeres to see if HP1α enrichment confers telomere deprotection. Strikingly, we found that enrichment of HP1α at telomeres led to an increase in the number of TIFs per cell more than five-fold compared to the wild type and non-induced conditions (Figure 7B, left panel). Surprisingly, we also noted the presence of entanglements, or telomere bridging, in which telomeres extend from one nucleus to another (figure 7A and 7B right panel). These fusions are especially notable because they are absent in our control conditions, and typically are observed in ALT+ cells as a byproduct of incompletely processed

intermediates during telomeric recombination. The appearance of this phenotype in our non-ALT HeLa cells with HP1α suggests that HP1α enrichment has a significant destabilizing effect on telomere end-processing.

Our IF-FISH analysis of the TRF1-HP1α condition also revealed a distinctly dimmed telomere signal throughout some cell nuclei compared to our non-induced control, which displayed a consistently robust telomere signal. Because the PNA-FISH probes at telomeres are semiquantitative and can be used as a proxy for telomere length, the observed reduction in telomere probe intensity in our HP1α-enriched cells suggests rapid telomere shortening is occurring. This is further supported by the Telo-FISH assay performed on the HP1α clones that also shows decreased intensity of the telomere probe fluorescence, in addition to a significantly higher prevalence of free ends (Figure 8A and 8B, left panel). Free ends are typically an indication of rapid telomere loss, often due to replication stress. However, when quantifying fragile telomeres, which directly represent replication stress events, we found no significant changes in the TRF1-HP1α cells (Figure 8B, right panel). This conveys the possibility that either replication stress and telomere shortening are occurring independently, or that the replication stress is occurring faster than our three-day Dox induction time point allows us to visualize, and we are instead seeing the aftermath of telomere processing through the increase in free ends. Regardless, our findings demonstrate that HP1α enrichment at telomeres has profound impacts on the regulation of telomere stability regarding end protection and telomere length dynamics.

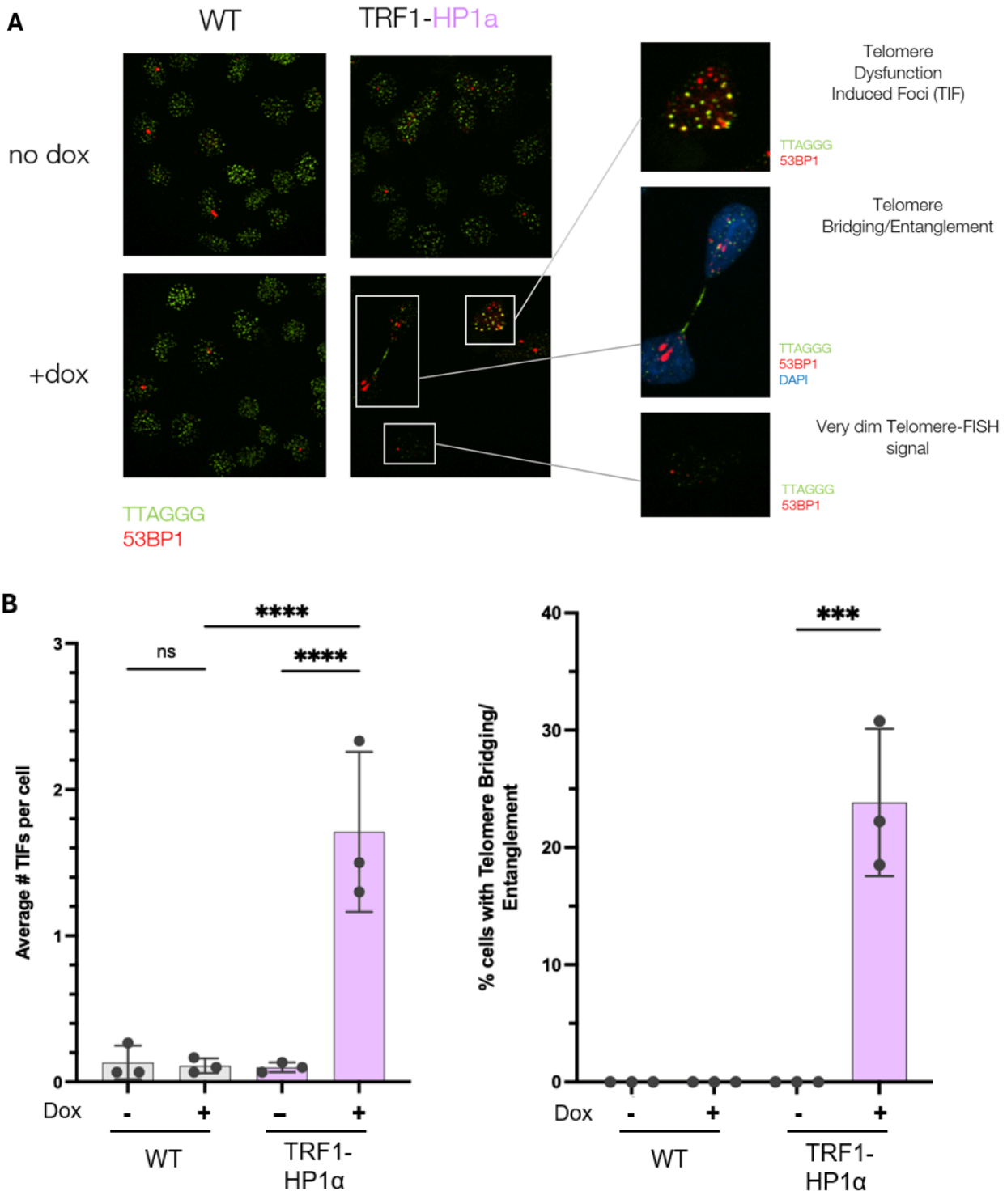


**Figure 7: HP1α enrichment results in significant DNA damage signalling and telomere instability.** (A) Immunostaining of TRF1-HP1α cells show increased TIFs, as well as telomere entanglements and dimmed Telo-C signal, indicating HP1α be detrimental to telomere end protection and length maintenance. (B) Quantifications of average TIFs per cell (left) and entanglements per cell (right) across all conditions.

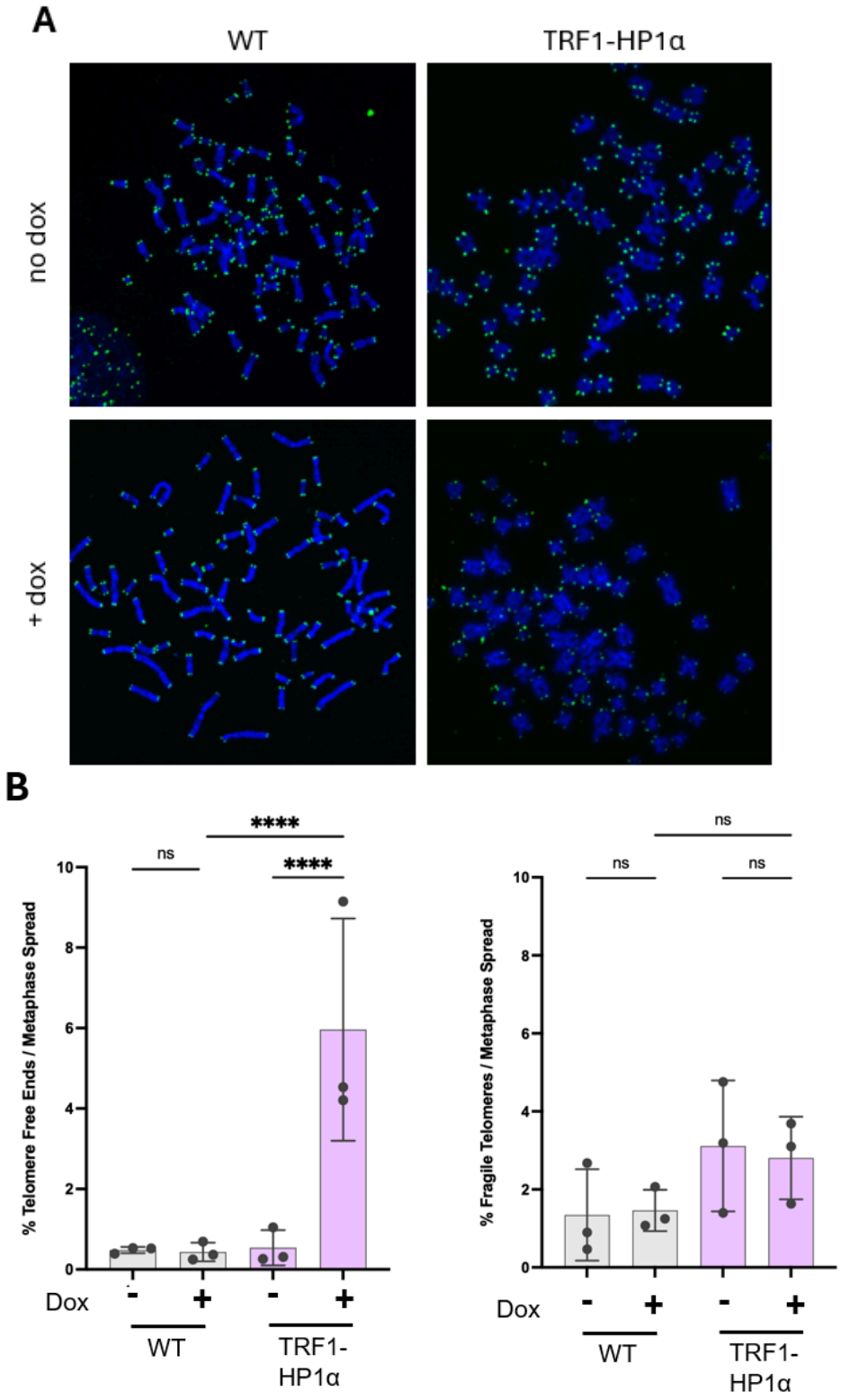


**Figure 8: Rapid telomere shortening upon HP1α enrichment further supported by replication stress assay.** (A) Representative images of Telo-FISH replication stress assay on TRF1-HP1α conditions. (B) Left: Quantification of free ends shows drastic increase in rapid telomere loss due to HP1α enrichment. Right: No significant changes observed in fragile telomere quantifications.

## DISCUSSION

While the function of the shelterin complex in the regulation of telomere length and stability has been well-characterized for decades, the potential role of telomeres' singular chromatin structure remains unclear. Our project sought to investigate the regulatory function of heterochromatin at telomeres, first through H3K9me3 enrichment by the KRAB minimal domain, followed by enrichment of heterochromatin-associated protein HP1α. Cells with increased presence of HP1α displayed higher levels of DNA damage signaling at telomeres, as well as increased hallmarks of telomere instability, including telomere bridging and rapid telomere shortening. This phenotype, in parallel with the null results from our TRF1-KRAB experiments, suggests that it is not the density of H3K9me3, but rather the presence of HP1α and its interactions with H3K9me3, that mediates a detrimental effect on telomere length maintenance and end-protection.

We initially hypothesized that because KRAB-mediated H3K9me3 upregulation had no effect in telomerase-positive HeLa cells, HP1α enrichment also would not have an effect at telomeres. Our results provided unexpected evidence to refute this hypothesis, as demonstrated by the TRF1-HP1α phenotype described above. Though surprising, the observed outcomes of this study align with a 2019 publication proposing that SETDB1-mediated enrichment of heterochromatin is associated with increased replication stress and the appearance of ALT features in non-ALT cells (Gauchier 2019). The authors assert that SETDB1-dependent heterochromatinization plays an essential role in regulating ALT, implying that it has a significant effect on telomere length and deprotection. Our study's findings support this claim. Since heterochromatin modulation by H3K9me3 enrichment alone did not produce DNA damage or replication stress in our, there may be mechanisms in place that prevent the recruitment and binding of additional heterochromatic

factors cannot be recruited. We speculate that enrichment of H3K9me3 density is insufficient to upregulate HP1α occupancy and destabilize telomeres in non-ALT cells. By this proposed model, only enrichment of HP1α is sufficient to bypass this mechanism of preventing heterochromatinization and cause a telomere deprotection and length dysregulation phenotype. If this is the case, our findings suggest that normal human, non-ALT cells are not only not enriched in heterochromatin, but may actively restrict enrichment of heterochromatin by certain regulatory mechanisms.

Moreover, within the TRF1-HP1α phenotype, it is notable that we only observed a substantial difference in free ends at telomeres, while we saw no such change in fragile telomeres. The fact that only one of these characteristics was affected by HP1α enrichment suggests one of two possibilities. One potential explanation is that replication stress occurs independently of rapid telomere loss and there is a separate mechanism (i.e. exonuclease activity) involved in telomere processing. We postulate that the increased prevalence of free ends may result fromdirect processing of telomere entanglements, rather than the processing of stalled or collapsed replication forks due to replication stress. Alternatively, replication stress could be occurring very rapidly after Dox induction, and our three-day collection point is too late to visualize fragile telomeres; instead, we could be seeing its consequence of rapid telomere loss in the form of free ends. To resolve this uncertainty, future directions for this work would include repeating the TRF1-HP1α experiment within a shorter time course, where cell samples are collected one day after induction to analyze and compare telomere structure by the Telo-FISH replication stress assay.

In contrast to our findings, a study in human bladder cancer UM-UC3 cells proposes that HP1α serves a protective function at telomeres rather than the adverse effect we observe. The authors show that HP1α tethering at telomeres produces a slight local enrichment in H3K9me3, but they provide evidence indicating that telomerase extension and experimentally-induced DNA damage at telomeres are attenuated by the expression of TRF1-HP1α (Chow 2018). They posit that the observed reduction in TIFs in artificially damaged cells with HP1α supports their claim that upregulated heterochromatin protects damaged telomeres. This is a stark contradiction from our observations in TRF1-HP1α cells, and while the reason for the discrepancy is unclear, it underscores the necessity for continued investigation into the functions of heterochromatin at telomeres.

Elucidating the molecular basis of our findings will require further investigation of HP1α and its mechanistic interactions specifically at telomeres. The semiquantitative nature of the telomere-binding PNA probe used in our TIF and replication stress assays served as a strong proxy for telomere length and structure but remains an approximation rather than a fully quantitative analysis. To substantiate our results and more accurately quantify the actual length of telomeres, future experiments should complement our analysis with telomere restriction fragment analysis (TRF analysis) which is considered the gold standard for telomere length analysis. The study could also benefit from supplemental analysis of HP1α mutants to differentiate the various domains and functions of HP1α and the specific effects of each on heterochromatin states and overall telomere dynamics. By this method, we may uncover further insight into the specific mechanisms that mediate the phenotypes we observe here, as well as additional information about other potential factors that may contribute to heterochromatin

formation and its involvement in the regulation of telomere function. In light of the previously established associations of heterochromatic upregulation specifically in human ALT cells, future investigations may benefit from further characterizing the ALT-like state exhibited by HP1α enrichment. A deeper analysis of the relationship between the high levels of telomere dysfunction observed in this study of non-ALT cells and the highly recombinogenic mechanisms of ALT may provide more context as to the specific involvement of HP1α in promoting an ALT-like state and reveal the mechanistic actions of HP1α binding and heterochromatin modulation that induce telomere dysfunction.

We conclude that upregulated heterochromatin by enrichment of HP1α at telomeres does not protect, but rather detracts from telomere stability, specifically regarding DNA damage signaling and telomere length dynamics. Our findings may have broader implications for the role of heterochromatin in promoting an ALT-like state in cancer development. Continued progress in this line of study may reveal new insights into the interplay between heterochromatin and ALT and new strategies for epigenetic intervention anti-cancer drug development.

## METHODS

### Plasmids, cell cloning, and tissue culture

For H3K9me3 enrichment, TRF1, a telomere-specific gene, was fused to our gene of interest, KRAB, which encodes for the recruitment of proteins responsible for the trimethylation of H3 histones at telomeres. A second plasmid fused TRF1 to a KRAB-mutant negative control, and a third plasmid contained TRF1 alone as a second control. For our following experiment with HP1α enrichment, TRF1 was directly fused to HP1α, a reader for H3K9me3. All plasmids

included a doxycycline promoter and a Myc tag on the N-terminus of TRF1 to allow all fusion proteins to be detected using the same antibody. Insertion of an autocleaving t2a-mCherry NES to verify induction levels of the fusion protein was done following the IN-fusion protocol by Takara Bio Inc. The lentiviral backbone vector, including the doxycycline-inducible constructs, contained 15bp overlaps complementary to the ends of a synthesized gene block that encodes the t2a-mcherryNES. This reporter sequence was inserted into all constructs, transformed into competent bacterial cells, and isolated using the Qiagen Miniprep protocol.

HeLa cell lines were transduced for fusion protein expression by standard lentiviral infection. Hek 293T cells were transfected with plasmids. Transfected cells were incubated for 72 hours in DMEM media with 10mM HEPES then harvested and transduced in target HeLa cells with polybrene (10ug/mL final concentration). Target cells were incubated with lentivirus for 48 hours, then selected with 1 ug/mL puromycin. Single clones were isolated by diluting cells in media and seeding them to have statistically one cell per two wells in a 96-well plate. Once individual colonies formed, expression of the fusion construct was verified by western blot and induction levels were quantified once more by flow cytometry. Clonal populations were selected to have equivalent expression levels across conditions.

Cells were cultured in 1X DMEM media supplemented with 1% penicillin-streptomycin, 1% non-essential amino acids, and 10% bovine calf serum. For +Dox conditions, 0.5ug/mL doxycycline was maintained in media at 1:2000 volume concentration for 72 hours before collection.

**Western Blotting**

Cells in culture were trypsinized, then spun and washed with PBS multiple times to remove trypsin and DMEM. The cells were transferred to microcentrifuge tubes and spun at 500g for 3 minutes at $4^0$C. The pellets were resuspended in a solution of 2X RIPA (equal volume to pellet size for 1X final), 1X Anti-protease, and 1uL/100uL Benzonase. All samples were incubated on ice for 30 minutes, with agitation by vortex every 10 minutes, 3 times total. The cells were centrifuged at 14,000 rpm for 30 min at $4^0$C. The supernatant was transferred to a new tube and protein concentrations were measured by bicinchoninic acid assay (BCA).

Page gel samples were prepared by adding 20 ug protein from cell lysates to 4X LDS buffer (1X final conc.) and 10X DTT (1X final conc.). The samples were then boiled in the ThermoMixer for 5 min at $85^0$C. Meanwhile, the gel box was filled with 1X SDS and the gel was inserted into the box. The samples were loaded into the wells of the gel along with 6uL of the PAGE RULER protein ladder, and the gel was run at 150V for 1 hour, or until all protein ran to the bottom of the gel. The gel was drained and rinsed with dH2O, then moved into a transfer box and prepared for transfer onto a nitrocellulose membrane. The transfer was run at 20V for 2 hours in 1X transfer buffer. After ensuring the PAGE RULER ladder correctly transferred onto the membrane, the membrane was stained with Ponceau to check for banding then rinsed with 1X TBST and cut to size to separate the bands for Myc-tagged TRF1, H3K9me3, and β-actin loading control. The separated membranes were washed with TBST on a shaker 3 more times, 5 min each.

To prepare for immunoblotting, the membrane was blocked with 5% milk in TBST for 30 min on the shaker at room temperature. The membranes were then incubated with their respective

primary antibody: Myc (mouse, 1:500), H3K9me3 (rabbit, 1:3000), or β-actin (rabbit, 1:1000) diluted in 5% milk ($4^0$C, overnight on shaker). The next day, the milk was poured off, the membranes were washed 3 times with TBST, and HRP-conjugated secondary antibodies (1:5000) were added for 45 min at room temperature. The secondary antibodies were anti-mouse or anti-rabbit, based on the animal in which the primary antibody was raised. The blots were washed three more times with TBST, then incubated with Femto/Dura for 2 min and visualized on Gbox.

**Immunofluorescence - fluorescence in-situ hybridization (IF-FISH)**

Cells were cultured on ethanol-sterilized coverslips at a concentration of approximately 50,000 cells per coverslip in a 24-well plate, then pre-extracted with CSK buffer for 7 minutes on ice and incubated with 2% paraformaldehyde in PBS for 10 minutes at room temperature. Coverslips were permeabilized in 1x KCM for 10 minutes, blocked with 100 ug/mL RNAse diluted in antibody dilution buffer (ABDIL), then overlaid with 1:1000 53BP1 anti-rabbit and 1:2000 Myc anti-mouse primary antibodies diluted in ABDIL for 1 hour at room temperature. This was followed by 3 five-minute PBST washes, incubation in secondary antibodies Alexafluor 568 and Alexafluor 647 for 30 minutes, 3 more PBST washes, and a second fixation in 2% paraformaldehyde for 10 minutes at room temperature. Coverslips were successively dehydrated, denatured at 84°C for 5 minutes, and hybridized in 2 ng/mL Telo-C PNA probe for 3 hours. Coverslips were washed with 70% formamide and 10mM Tris-HCl (pH 7.5) three times for 5 minutes each, then with a solution of 50mM Tris-HCl (pH7.5), 150 mM NaCl and .05% Tween20 three times for 5 minutes each. The coverslips were air-dried and mounted onto slides

with Vectashield+DAPI. Images were visualized using the Nikon Ti Eclipse spinning disk confocal microscope.

**Telomere fluorescence in-situ hybridization (Telo-FISH)**

Metaphase spreads were prepared by standard procedure. Growing cells were arrested in metaphase by 0.1 ug/mL colcemid incubation for 3 hours, collected, swollen in 75 mM KCl for 10 minutes at 37°C, and fixed with a 3:1 solution methanol:glacial acetic acid three times, the first being on gentle agitation. Metaphases were dropped onto slides and dried overnight. Slides were re-hydrated in PBS, fixed for 2 minutes in 3.7% formaldehyde, digested in 1mg/mL pepsin at 37℃ for 10 minutes, then fixed again for 2 minutes in 3.7% formaldehyde, and washed in PBS. After slides were successively dehydrated with 70%, 90%, and 100% ethanol, Telo-C and Centromere probes diluted in PNA Hybridization Buffer with blocking reagent were applied, and slides underwent a 5 min denaturation at 84°C and overnight hybridization at room temperature. Slides were washed with 70% formamide and 10mM Tris-HCl (pH 7.5) three times for 5 minutes each, then with a solution of 50mM Tris-HCl (pH7.5), 150 mM NaCl, and .05% Tween20 three times for 5 minutes each. Slides were incrementally dehydrated in 70%, 90%, and 100% ethanol for 3 minutes each, then stained and mounted with Vectashield + DAPI. The slides were imaged using the Yokogawa & Olympus Cell Voyager CV1000 spinning disk confocal microscope using a 100x oil immersion objective.

**Image quantification and statistical analysis**

All images were analyzed using Fiji ImageJ software with a custom macro to automate image pre-processing. Quantification was performed manually, blinded to conditions to reduce bias. All figures and statistical analyses were performed using GraphPad Prism software.

REFERENCES

Arnoult, N., Karlseder, J. Complex interactions between the DNA-damage response and mammalian telomeres. Nat Struct Mol Biol 22, 859–866 (2015). https://doi.org/10.1038/nsmb.3092

Azzalin CM, Reichenbach P, Khoriauli L, Giulotto E, Lingner J. Telomeric repeat containing RNA and RNA surveillance factors at mammalian chromosome ends. Science. 2007 Nov 2;318(5851):798-801. doi: 10.1126/science.1147182. Epub 2007 Oct 4. PMID:17916692.

Bonnell E, Pasquier E, Wellinger RJ. Telomere Replication: Solving Multiple End Replication Problems. Front Cell Dev Biol. 2021 Apr 1;9:668171. doi: 10.3389/fcell.2021.668171. PMID: 33869233; PMCID: PMC8047117.

Cesare, A., Reddel, R. Alternative lengthening of telomeres: models, mechanisms and implications. Nat Rev Genet 11, 319–330 (2010). https://doi.org/10.1038/nrg2763

Chan, SL., Blackburn, E. New ways not to make ends meet: telomerase, DNA damage proteins and heterochromatin. Oncogene 21, 553–563 (2002). https://doi.org/10.1038/sj.onc.1205082

Chow, T.T., Shi, X., Wei, JH. et al. Local enrichment of HP1alpha at telomeres alters their structure and regulation of telomere protection. Nat Commun 9, 3583 (2018). https://doi.org/10.1038/s41467-018-05840-y

Cubiles MD, Barroso S, Vaquero-Sedas MI, Enguix A, Aguilera A, Vega-Palas MA. Epigenetic features of human telomeres. Nucleic Acids Res. 2018 Mar 16;46(5):2347-2355. doi: 10.1093/nar/gky006. PMID: 29361030; PMCID: PMC5861411.

de Lange T. How telomeres solve the end-protection problem. Science. 2009 Nov 13;326(5955):948-52. doi: 10.1126/science.1170633. PMID: 19965504; PMCID:

PMC2819049.

de Lange, T. Shelterin: the protein complex that shapes and safeguards human telomeres. Genes Dev. 19, 2100–2110 (2005). https://genesdev.cshlp.org/content/19/18/2100.full

Emerson, R. O., & Thomas, J. H. (2009). Adaptive evolution in zinc finger transcription factors. PLOS Genetics, 5(1), e1000325. https://doi.org/10.1371/journal.pgen.1000325

ESMO Oncology Pro. 2024. Replication stress and cancer. https://oncologypro.esmo.org/oncology-in-practice/anti-cancer-agents-and-biological-therapy/parp-inhibition-and-dna-damage-response-ddr/dna-damage-response/ddr-in-cancer

Gaillard, H., García-Muse, T. & Aguilera, A. Replication stress and cancer. Nat Rev Cancer 15, 276–289 (2015). https://doi.org/10.1038/nrc3916

Gauchier, M. et al. SETDB1-dependent heterochromatin stimulates alternative lengthening of telomeres. Sci. Adv.5,eaav3673(2019).DOI:10.1126/sciadv.aav3673

Guterres, A.N., Villanueva, J. Targeting telomerase for cancer therapy. Oncogene 39, 5811–5824 (2020). https://doi.org/10.1038/s41388-020-01405-w

HealthJade. (2024) Telomerase. Retrieved from https://healthjade.net/telomerase/

Janssen, A., Colmenares, S. U., & Karpen, G. H. (2018). Heterochromatin: Guardian of the Genome. Annual Review of Cell and Developmental Biology, 34, 265-288. https://doi.org/10.1146/annurev-cellbio-100617-062653

Li A, Cartwright S, Yu A, Ho SM, Schrode N, Deans PJM, Matos MR, Garcia MF, Townsley KG, Zhang B, Brennand KJ. Using the dCas9-KRAB system to repress gene expression in hiPSC-derived NGN2 neurons. STAR Protoc. 2021 Jun 3;2(2):100580. Doi: 10.1016/j.xpro.2021.100580. PMID: 34151300; PMCID: PMC8188621.

Lu R, Pickett HA. Telomeric replication stress: the beginning and the end for alternative

lengthening of telomeres cancers. Open Biol. 2022 Mar;12(3):220011. Doi: 10.1098/rsob.22001. Epub 2022 Mar 9. PMID: 35259951; PMCID: PMC8905155.

Oeseburg H, de Boer RA, van Gilst WH, van der Harst P. Telomere biology in healthy aging and disease. Pflugers Arch. 2010 Jan;459(2):259-68. doi: 10.1007/s00424-009-0728-1. Epub 2009 Sep 10. PMID: 19756717; PMCID: PMC2801851.

Roake CM, Artandi SE. Regulation of human telomerase in homeostasis and disease. Nat Rev Mol Cell Biol. 2020 Jul;21(7):384-397. doi: 10.1038/s41580-020-0234-z. Epub 2020 Apr 2. PMID: 32242127; PMCID: PMC7377944.

Rose AM, Goncalves T, Cunniffe S, Geiller HEB, Kent T, Shepherd S, Ratnaweera M, O'Sullivan RJ, Gibbons RJ, Clynes D. Induction of the alternative lengthening of telomeres pathway by trapping of proteins on DNA. Nucleic Acids Res. 2023 Jul 21;51(13):6509-6527. doi: 10.1093/nar/gkad150. PMID: 36940725; PMCID: PMC10359465.

Sfeir A, Kosiyatrakul ST, Hockemeyer D, MacRae SL, Karlseder J, Schildkraut CL, de Lange T. Mammalian telomeres resemble fragile sites and require TRF1 for efficient replication. Cell. 2009 Jul 10;138(1):90-103. doi: 10.1016/j.cell.2009.06.021. PMID: 19596237; PMCID: PMC2723738.

Shay, J.W., Wright, W.E. Telomeres and telomerase: three decades of progress. Nat Rev Genet 20, 299–309 (2019). https://doi.org/10.1038/s41576-019-0099-1

Shen, M., Young, A,. Autexier, C. PCNA, a focus on replication stress and the alternative lengthening of telomeres pathway, DNA Repair, Volume 100, 2021, 103055, ISSN 1568-7864, https://doi.org/10.1016/j.dnarep.2021.103055.

Soman, A., Wong, S.Y., Korolev, N. et al. Columnar structure of human telomeric chromatin.

Nature 609, 1048–1055 (2022). https://doi.org/10.1038/s41586-022-05236-5

Tan J, Lan L. The DNA secondary structures at telomeres and genome instability. Cell Biosci. 2020 Mar 26;10:47. doi: 10.1186/s13578-020-00409-z. PMID: 32257105; PMCID: PMC7104500.

Vaquero-Sedas MI, Vega-Palas MA. On the chromatin structure of eukaryotic telomeres. Epigenetics. 2011 Sep 1;6(9):1055-8. doi: 10.4161/epi.6.9.16845. Epub 2011 Sep 1. PMID: 21822057; PMCID: PMC3225743.

Xu, J., Ma, H., Ma, H. et al. Super-resolution imaging reveals the evolution of higher-order chromatin folding in early carcinogenesis. Nat Commun 11, 1899 (2020). https://doi.org/10.1038/s41467-020-15718-7

Yang Z, Takai KK, Lovejoy CA, de Lange T. Break-induced replication promotes fragile telomere formation. Genes Dev. 2020 Oct 1;34(19-20):1392-1405. Doi: 10.1101/gad.328575.119. Epub 2020 Sep 3. PMID: 32883681; PMCID: PMC7528700.

Zhang JM, Zou L. Alternative lengthening of telomeres: from molecular mechanisms to therapeutic outlooks. Cell Biosci. 2020 Mar 10;10:30. doi: 10.1186/s13578-020-00391-6. PMID: 32175073; PMCID: PMC7063710.